SCIENCE CHINA
Information Sciences

• RESEARCH PAPER •

September 2022, Vol. 65 192202:1–192202:13
https://doi.org/10.1007/s11432-020-3153-x

Disturbance observer-based nonsingular fixed-time sliding mode tracking control for a quadcopter

Xing CHENG[1], Zhi-Wei LIU[1*], Huazhou HOU[2] & Zhi-Hong GUAN[1]

[1]*School of Artificial Intelligence and Automation, State Key Laboratory of Digital Manufacturing Equipment and Technology, Huazhong University of Science and Techology, Wuhan* 430074*, China;*
[2]*School of Automation, Southeast University, Nanjing* 211189*, China*

Received 9 May 2020/Revised 30 September 2020/Accepted 1 December 2020/Published online 25 August 2022

Abstract This paper proposes a fixed-time method for the tracking control of a quadcopter subject to external disturbances. Compared with finite-time tracking control, the proposed control strategy ensures that the upper bound of the convergence time is independent of the initial state of the system. To determine the external disturbances, we have designed a fixed-time disturbance observer (FTDO). This allows the external disturbances to be compensated precisely, as a result of which the robustness of the control algorithm is enhanced, and the chattering problem is alleviated. We also propose a novel nonsingular fixed-time sliding mode control (FTSMC) technique to provide fixed-time position and attitude tracking control for the quadcopter, which enables a more accurate determination of the convergence time. We validated the fixed-time convergence of the proposed quadcopter tracking control method using Lyapunov stability theory. Finally, we verified the theoretical results not only by simulations but also by experiments.

Keywords fixed-time disturbance observer (FTDO), fixed-time sliding mode control (FTSMC), quadcopter, trajectory tracking, nonsingular

Citation Cheng X, Liu Z-W, Hou H Z, et al. Disturbance observer-based nonsingular fixed-time sliding mode tracking control for a quadcopter. Sci China Inf Sci, 2022, 65(9): 192202, https://doi.org/10.1007/s11432-020-3153-x

1 Introduction

Quadcopters are now widely employed in various fields due to their flexibility, including the capability for fast response. Future quadcopters are expected to require significantly faster and more accurate time responses to position and attitude tracking commands, which is key for better performance in scenarios such as flight racing and acrobatic maneuvering. However, the designed controllers in most of the existing literature only promise asymptotic convergence [1, 2] or finite-time convergence [3–6]. Asymptotic convergence means that it requires infinite time for the state of a quadcopter to converge to the equilibrium point. On the other hand, finite-time convergence means that an upper bound to the convergence time can be obtained, but that it varies with system's initial state. As a result, the aforementioned future expectations can hardly be satisfied. Fortunately, a new concept, called fixed-time convergence, first proposed by Polyakov [7], has emerged as the solution to the aforementioned high-performance trajectory tracking problem. Compared with finite-time convergence, the upper bound to the settling time for fixed-time convergence is only determined by the design parameters, regardless of the initial conditions. Consequently, the convergence time for fixed-time control can be minimized to a constant, independent of the initial state, and it can be limited to a more accurate boundary. Due to these advantages, the fixed-time control algorithm promises to provide faster and more accurate time response, and it has become an extensively studied theory in recent years. For example, Ref. [8] has proposed a global fixed-time stabilization strategy for a class of dynamic non-holonomic systems, using one power integrator and terminal sliding mode control. Further, Ref. [9] presented a nonlinear control protocol that solved the problem of exact average-consensus reaching in a pre-specified time. In

* Corresponding author (email: zwliu@hust.edu.cn)

addition, Ref. [10] investigated the locally fixed-time and globally fixed-time $\mathcal{H}_\infty$ control problems for port-controlled Hamiltonian systems.

However, the application of fixed-time control to second-order systems is often faced with singularity problems [11]. Although some investigations [11–13] have developed methods to eliminate singularity problems, the design of a nonsingular, fixed-time controller is of high computational complexity, and determinations of the convergence time are rather conservative, which may be unacceptable in some cases [14]. In addition, there exist conflicts between disturbance resistance and chattering suppression in the input signals. For instance, to resist disturbances, Refs. [12,15,16] introduced a switching signal into the control inputs, which caused great chattering in the input signals and restricted practical applications of this control scheme.

Designing a disturbance observer to compensate for the disturbances is another important anti-disturbance method. Many kinds of disturbance observers have been designed, and they have been applied to solve different kinds of control problems for various complex systems. A sliding mode disturbance observer was designed in [17] to determine unknown external disturbances in a nonlinear MIMO system. Huang et al. [18] proposed a high-order disturbance observer based on a choice method that utilizes optimal gain matrices to improve the performance. For more detail about disturbance-observer-based control, the reader can refer to the survey in [19]. In recent years, some scholars have applied the disturbance-observer method to solve the control problem of a quadcopter subject to a disturbance. For example, a disturbance observer was designed in [20] to compensate for slowly time-varying disturbances in the quadcopter tracking control problem. In [21], an observer-based fault-determination method was proposed for the quadcopter take-off mode. However, these approaches can only ensure that the closed-loop systems converge asymptotically or in a finite time.

In this paper, we propose a novel fixed-time trajectory tracking control using a fixed-time disturbance observer for tracking control of the quadcopter. We analyze the fixed convergence of the closed-loop system strictly using Lyapunov stability theory. The main contributions are twofold. First, to suppress the influence of uncertainty, as well as to alleviate the chattering, we introduce disturbance determination by the proposed fixed-time disturbance observer, instead of using switching signals in the control inputs. Second, compared with [15], the proposed fixed-time, trajectory-tracking control approach, which is both nonsingular and of simpler form, determines the convergence time more accurately. Furthermore, we verified the theoretical results not only by simulations but also by experiments.

The layout of this paper is as follows. The notations, definitions, and lemmas concerning fixed-time stability are recalled in Section 2. In Section 3, the quadcopter model is presented. Section 4 formulates the design of the controller and provides the stability analysis. The simulations and experimental results are discussed in Section 5. Section 6 presents the conclusion.

2 Preliminaries

2.1 Notations

The following notations will be used throughout this paper. Let $\|x\| = \sqrt{x^{\mathrm{T}}x}$ be the Euclidean norm of vector x, where $x = [x_1, \ldots, x_n]^{\mathrm{T}}$. Let $\mathrm{sgn}(x) = [\mathrm{sgn}(x_1), \ldots, \mathrm{sgn}(x_n)]^{\mathrm{T}}$, $|x| = [|x_1|, \ldots, |x_n|]^{\mathrm{T}}$, $\int_0^t x\mathrm{d}\tau = [\int_0^t x_1\mathrm{d}\tau, \ldots, \int_0^t x_n\mathrm{d}\tau]^{\mathrm{T}}$ and $x^{\mathrm{c}} = [x_1^{\mathrm{c}}, \ldots, x_n^{\mathrm{c}}]^{\mathrm{T}}$, where c is a constant. Given a vector $y = [y_1, \ldots, y_n]^{\mathrm{T}}$, one has $x \circ y \triangleq [x_1y_1, \ldots, x_ny_n]^{\mathrm{T}}$.

2.2 Definitions and Lemmas

Consider the system

$$\dot{x} = f(x,t), \quad x(0) = x_0, \quad f(0,t) = 0, \tag{1}$$

where $x \in \mathbb{R}^n$, $f : \mathbb{R}^n \to \mathbb{R}^n$ is a nonlinear function.

Definition 1 ([7])**.** The system (1) is said to be globally finite-time stable if it is globally asymptotically stable and any solution of (1) reaches the equilibrium point at some finite time moment, i.e., $x(t) = 0$, $\forall t \geqslant T(x_0)$, where T is the settling-time function.

Definition 2 ([7])**.** The system (1) is said to be globally fixed-time stable if it is globally asymptotically stable and the settling-time function $T(x_0)$ is bounded, i.e., $\exists T_{\max} > 0 : T(x_0) \leqslant T_{\max}$.

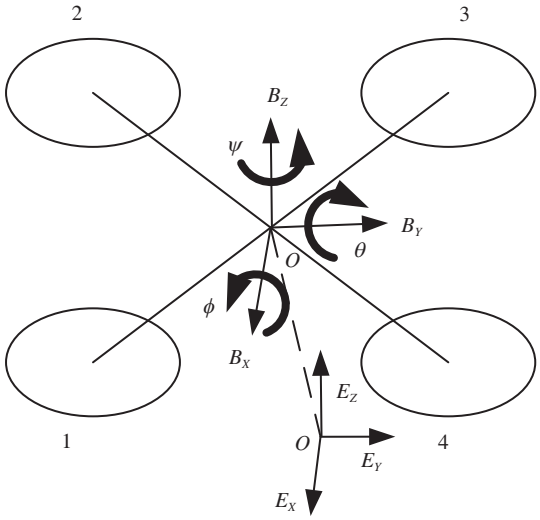

Figure 1 The structure of a typical quadcopter.

Lemma 1 ([7]). For system (1), suppose there exists a positive definite function $V(x) : \mathbb{R}^n \to \mathbb{R}$ such that $\dot{V}(x) \leqslant -(\alpha V^p(x) + \beta V^q(x))^k$, where $\alpha > 0$, $\beta > 0$, $p > 0$, $q > 0$, and $pk < 1$, $qk > 1$. Then the origin of the system (1) is fixed-time stable and the settling time T is bounded by $T \leqslant 1/(\alpha^k(1-pk)) + 1/(\beta^k(qk-1))$.

Lemma 2 ([13]). Let $x_1, x_2, \ldots, x_n \geqslant 0$ and $p > 1$. Then

$$\sum_{i=1}^{n} x_i^p \geqslant n^{1-p}\left(\sum_{i=1}^{n} x_i\right)^p.$$

Lemma 3 ([13]). Let $x_1, x_2, \ldots, x_n \geqslant 0$ and $0 < l < 1$. Then

$$\sum_{i=1}^{n} x_i^l \geqslant \left(\sum_{i=1}^{n} x_i\right)^l.$$

3 Quadcopter model

The structure of a quadcopter considering in this paper is depicted in Figure 1. At each extremity of its four arms is a rotor attached with a propeller. By adjusting the angular rate of each propeller the quadcopter can perform translational and rotational motions. Let $E = \{E_x, E_y, E_z\}$ and $B = \{B_x, B_y, B_z\}$ be the body-fixed frame and the earth-fixed frame respectively, as shown in Figure 1. $p = [x, y, z]^{\mathrm{T}}$ and $v = [v_x, v_y, v_z]^{\mathrm{T}}$ denote the position and velocity vector of the center of gravity of the quadcopter in frame E, respectively. $\Theta = [\phi, \theta, \psi]^{\mathrm{T}}$ is the Euler angle. $\Omega = [\omega_x, \omega_y, \omega_z]^{\mathrm{T}}$ is the angular velocity vector in the body-fixed frame. The rotation matrix that associates the body-fixed frame B with the earth-fixed frame E is

$$R = \begin{bmatrix} C_\theta C_\psi & C_\psi S_\phi S_\theta - C_\phi S_\psi & S_\phi S_\psi + C_\phi C_\psi S_\theta \\ C_\theta S_\psi & C_\phi C_\psi + S_\phi S_\theta S_\psi & C_\phi S_\theta S_\psi - C_\psi S_\phi \\ -S_\theta & C_\theta S_\phi & C_\phi C_\theta \end{bmatrix},$$

where $C_\bullet = \cos(\bullet)$ and $S_\bullet = \sin(\bullet)$. The translational and rotational dynamics of the quadcopter [4] can be described using the following equations:

$$\dot{p} = v, \tag{2}$$

$$\dot{v} = -gE_z + \frac{u_1}{m} RE_z + D_1, \tag{3}$$

$$\dot{\Theta} = W\Omega, \tag{4}$$

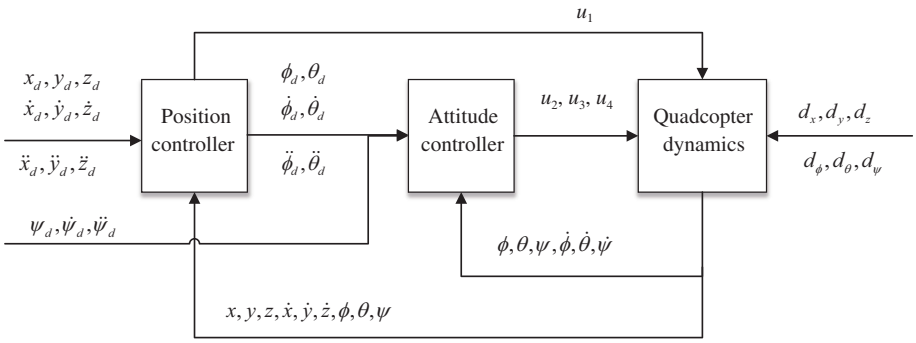

Figure 2 Dual loop structure of the control system.

$$\dot{\Omega} = -I^{-1}\Omega \times I\Omega + I^{-1}M + D_2, \tag{5}$$

where

$$W = \begin{bmatrix} 1 & \sin\phi\tan\theta & \cos\phi\tan\theta \\ 0 & \cos\phi & -\sin\phi \\ 0 & \sin\phi\sec\theta & \cos\phi\sec\theta \end{bmatrix},$$

m is the quadcopter's total mass, g is gravitational acceleration, $E_z = [0, 0, 1]^{\mathrm{T}}$ is a unit vector, u_1 is the total thrust, $M = [u_2, u_3, u_4]^{\mathrm{T}}$ is the control torque and $I = \mathrm{diag}(I_{xx}, I_{yy}, I_{zz})$ is the inertia matrix relative to B. The terms $D_1 = [d_x, d_y, d_z]^{\mathrm{T}}$ and $D_2 \in \mathbb{R}^3$ represent unmodeled parts, system uncertainties or external disturbances.

Remark 1. The relationship between u_1, u_2, u_3, and u_4 and angular rate of each propeller, i.e., ω_1, ω_2, ω_3, and ω_4 is given by

$$\begin{bmatrix} w_1^2 \\ w_2^2 \\ w_3^2 \\ w_4^2 \end{bmatrix} = \frac{1}{4a} \begin{bmatrix} 1 & -\frac{\sqrt{2}}{l} & -\frac{\sqrt{2}}{l} & -\frac{l}{b} \\ 1 & -\frac{\sqrt{2}}{l} & \frac{\sqrt{2}}{l} & \frac{l}{b} \\ 1 & \frac{\sqrt{2}}{l} & \frac{\sqrt{2}}{l} & -\frac{l}{b} \\ 1 & \frac{\sqrt{2}}{l} & -\frac{\sqrt{2}}{l} & \frac{l}{b} \end{bmatrix} \begin{bmatrix} u_1 \\ u_2 \\ u_3 \\ u_4 \end{bmatrix},$$

where a denotes the angular rate to force scaling factor and b denotes the force to moment scaling factor. Once u_1, u_2, u_3, and u_4 are given, ω_1, ω_2, ω_3, and ω_4 are determined by the above equation.

Remark 2. The system model of the quadcopter is very complicated. Beyond system uncertainties, there are many other difficulties to overcome. From (3), it is concluded that the attitude of the quadcopter affects its motion in the earth-fixed frame. In other words, the translational dynamics is strongly coupled with the rotational dynamics, leading to a fourth-order system. In addition, the motion of a quadcopter has six degrees of freedom (DOF), which is controlled only by four inputs. Therefore, the quadcopter is a typical underactuated system. All the above characteristics make the controller design of the quadcopter challenge.

4 Controller design and stability analysis

4.1 Control structure

The control objective of this paper is to design a feedback control u_1, u_2, u_3, and u_4 for a quadcopter to robustly track the desired position $x_d(t)$, $y_d(t)$, $z_d(t)$ and yaw angle $\psi_d(t)$, whose first and second derivatives are already known.

In order to solve the coupling problem of translation and rotation motion coupling, as well as underactuation problem, inspired by [22], the proposed controller is designed as a double loop structure as shown in Figure 2. The position controller is applied to the translational dynamics of the quadcopter, depicted

by (2) and (3), and outputs a virtual control signal $\tilde{U}_1$, which is defined as $\tilde{U}_1 = \frac{u_1}{m} R E_z = [\tilde{u}_1, \tilde{u}_2, \tilde{u}_3]^{\mathrm{T}}$, where

$$\tilde{u}_1 = (S_\phi S_\psi + C_\phi C_\psi S_\theta) u_1/m, \tag{6}$$
$$\tilde{u}_2 = (C_\phi S_\theta S_\psi - C_\psi S_\phi) u_1/m, \tag{7}$$
$$\tilde{u}_3 = C_\phi C_\theta u_1/m. \tag{8}$$

u_1 can be obtained by

$$u_1 = m\sqrt{\tilde{u}_1^2 + \tilde{u}_2^2 + \tilde{u}_3^2}. \tag{9}$$

Note that the desired roll angle ϕ_d and pitch angle θ_d cannot be obtained directly. They can be computed by

$$\begin{cases} \theta_d = \arctan((\tilde{u}_1 \cos\psi + \tilde{u}_2 \sin\psi)/\tilde{u}_3), \\ \phi_d = \arcsin((\tilde{u}_1 \sin\psi - \tilde{u}_2 \cos\psi) m/u_1). \end{cases} \tag{10}$$

In practice, we usually pay more attention to the position and velocity in the earth-fixed frame. As a result, the desired yaw angle ψ_d is usually set to zero. The attitude controller is applied to the rotational dynamics of the quadcopter, depicted by (4) and (5), and outputs the control signals u_2, u_3, u_4.

To deal with the disturbance problem, both the position controller and the attitude controller are developed with a disturbance observer.

Remark 3. By adopting the dual control loop structure, the complicated fourth-order system is decoupled and separated into two simpler second-order systems, making design control easier.

4.2 The position controller

Let $p_d = [x_d, y_d, z_d]^{\mathrm{T}}$, $e_p = p - p_d$, and $e_v = v - \dot{p}_d$. Then, from (2) and (3),

$$\begin{cases} \dot{e}_p = e_v, \\ \dot{e}_v = -gE_z + \tilde{U}_1 + D_1 - \ddot{p}_d. \end{cases} \tag{11}$$

Assumption 1. $d_i(0) = 0$, $|\dot{d}_i| \leqslant L_1$, $i \in \{x, y, z\}$, where $L_1 > 0$ is a constant.

4.2.1 *Design of the disturbance observer* $\hat{D}_1$

The disturbance observer is designed as

$$\hat{D}_1 = -k_3 \int_0^t \mathrm{sgn}(\Delta_1) \mathrm{d}\tau, \tag{12}$$

where $\Delta_1 = Y_1 - e_v = [\Delta_{11}, \Delta_{12}, \Delta_{13}]^{\mathrm{T}}$,

$$Y_1 = \int_0^t -k_1 \Delta_1 \|\Delta_1\|^{\mu_1 - 1} - k_2 \Delta_1 \|\Delta_1\|^{\lambda_1 - 1} + \hat{D}_1 - gE_z + \tilde{U}_1 - \ddot{p}_d \mathrm{d}\tau, \tag{13}$$

$k_1 > \sqrt{2k_3}$, $k_2 > 0$, $k_3 > 4L_1$, $0 < \mu_1 < 1$, and $\lambda_1 > 1$.

Define the estimation error as $\tilde{D}_1 = \hat{D}_1 - D_1 = [\tilde{D}_{11}, \tilde{D}_{12}, \tilde{D}_{13}]^{\mathrm{T}}$.

Theorem 1. Consider the system (11). Under Assumption 1 with the disturbance observer (12), $\tilde{D}_1$ will converge to zero in a fixed time

$$t_0 = t_{01} + t_{02}, \tag{14}$$

where

$$t_{01} \leqslant \frac{2^{(1-\mu_1)/2}}{k_1(1-\mu_1)} + \frac{2^{(1-\lambda_1)/2}}{k_2(\lambda_1 - 1)}, \tag{15}$$

and

$$t_{02} \leqslant \frac{k_3 + L_1}{(k_3 - L_1)(1 - \sqrt{2k_3}/k_1)} \left(\frac{2^{(1-\mu_1)/2}}{k_1(1-\mu_1)} + \frac{2^{(1-\lambda_1)/2}}{k_2(\lambda_1 - 1)} \right). \tag{16}$$

Proof. Differentiate Δ_1 and $\tilde{D}_1$ with respect to time, and we obtain

$$\dot{\Delta}_1 = -k_1\Delta_1\|\Delta_1\|^{\mu_1-1} - k_2\Delta_1\|\Delta_1\|^{\lambda_1-1} + \tilde{D}_1, \tag{17}$$

and

$$\dot{\tilde{D}}_1 = -k_3\mathrm{sgn}(\Delta_1) - \dot{D}_1. \tag{18}$$

Next, we discuss two cases.

Case 1. $\|\Delta_1\| \neq 0$. Multiply both sides of (17) by $\dfrac{\Delta_1^{\mathrm{T}}}{\|\Delta_1\|}$, and then

$$\frac{\mathrm{d}\|\Delta_1\|}{\mathrm{d}t} = -k_1\|\Delta_1\|^{\mu_1} - k_2\|\Delta_1\|^{\lambda_1} + \frac{\Delta_1^{\mathrm{T}}\tilde{D}_1}{\|\Delta_1\|}. \tag{19}$$

If $\Delta_{1i} = 0$, then $\Delta_{1i}\tilde{D}_{1i} = 0$. If $\Delta_{1i} > 0$, accrrding to Assumption 1 and (18), $\tilde{D}_{1i} < 0$, $\Delta_{1i}\tilde{D}_{1i} < 0$. If $\Delta_{1i} < 0$, we have $\tilde{D}_{1i} > 0$; thus $\Delta_{1i}\tilde{D}_{1i} < 0$. To conclude, if $\|\Delta_1\| \neq 0$, then $\dfrac{\Delta_1^{\mathrm{T}}\tilde{D}_1}{\|\Delta_1\|} < 0$. Define $s = \|\Delta_1\|$. Then the following inequality can be obtained:

$$\dot{s} \leqslant -k_1 s^{\mu_1} - k_2 s^{\lambda_1}. \tag{20}$$

Select the Lyapunov candidate function as $V = \frac{1}{2}s^2$. Then

$$\dot{V} = s\dot{s} \leqslant -k_1 s^{\mu_1+1} - k_2 s^{\lambda_1+1} = -k_1 2^{\frac{\mu_1+1}{2}} V^{\frac{\mu_1+1}{2}} - k_2 2^{\frac{\lambda_1+1}{2}} V^{\frac{\lambda_1+1}{2}}. \tag{21}$$

According to Lemma 3, $\|\Delta_1\| = 0$ in a fixed time t_{01}, whose upper bound is (15).

Considering (18) and Assumption 1, we have $|\dot{\tilde{D}}_{1i}| \in [0, k_3 + L_1]$, and taking into account $\hat{D}_1(0) = 0$, the upper bound of $|\tilde{D}_{1i}|$ at time t_{01} is obtained:

$$|\tilde{D}_{1i}(t_{01})| \leqslant (k_3 + L_1)t_{01}, \quad i \in \{1, 2, 3\}. \tag{22}$$

Case 2. $\|\Delta_1\| = 0$. In this case, following the proof of Theorem 2 in [14], the convergence time for this case is calculated as

$$t_{02} = |\tilde{D}_{1i}(t_{01})|/((k_3 - L_1)(1 - q_c)), \tag{23}$$

where the value of q_c can be estimated by

$$q_c = \sqrt{2k_3}/k_1. \tag{24}$$

Substituting (15), (22), and (24) into (23) yields (16). Note that t_{01} and t_{02} only rely on designed parameters k_1, k_2, k_3, μ_1, and λ_1.

Therefore, $\tilde{D}_1$ will converge to zero within a fixed time t_0 in (14). This concludes the proof.

Remark 4. Consider the term $\Delta_1\|\Delta_1\|^{\mu_1-1}$ in (13). If $\Delta_1 = \mathbf{0}$, then $\Delta_{1i}\|\Delta_1\|^{\mu_1-1} = \Delta_{1i}(\Delta_{1i}^2)^{\frac{\mu_1-1}{2}}$ $= \Delta_{1i}|\Delta_{1i}|^{\mu_1-1} = |\Delta_{1i}|^{\mu_1}\mathrm{sgn}(\Delta_{1i})$, $i = \{1, 2, 3\}$. Since $\mu_1 > 0$, $|\Delta_{1i}|^{\mu_1}\mathrm{sgn}(\Delta_{1i}) = 0$, $\Delta_1\|\Delta_1\|^{\mu_1-1} = \mathbf{0}$. Consequently, the term $\Delta_1\|\Delta_1\|^{\mu_1-1}$ is nonsingular.

4.2.2 *Design of the virtual control law* $\tilde{U}_1$

A fixed-time sliding mode surface is designed as the following form:

$$S_1 = e_v + \alpha_1(\beta_1\mathbf{1}_3 + e_p^2)^{\frac{3}{2}} \circ \mathrm{sgn}(e_p), \tag{25}$$

where $\alpha_1 > 0$, $\beta_1 > 0$, and $\mathbf{1}_3$ denotes vector $[1, 1, 1]^{\mathrm{T}}$.

$\tilde{U}_1$ can be designed as the form of

$$\tilde{U}_1 = \tilde{U}_{1eq} + \tilde{U}_{1*} - \hat{D}_1, \tag{26}$$

where

$$\tilde{U}_{1eq} = gE_z + \ddot{p}_d, \tag{27}$$

and

$$\tilde{U}_{1*} = -\alpha_2 S_1^{\frac{m_1}{n_1}} - \beta_2 S_1^{\frac{p_1}{q_1}} - 3\alpha_1(\beta_1\mathbf{1}_3 + e_p^2)^{\frac{1}{2}} \circ e_v \circ |e_p|, \tag{28}$$

where $\alpha_2 > 0$, $\beta_2 > 0$, $0 < n_1 < m_1$, $0 < p_1 < q_1$, m_1, n_1, p_1, and q_1 are odd numbers.

Theorem 2. If $\tilde{U}_1$ is designed as (12) and (26), with the fixed-time sliding mode surface (25), e_p and e_v will converge to zero in a fixed time. The convergence time is bounded by

$$t \leqslant t_0 + \frac{(3/2)^{(m_1-n_1)/(2n_1)} n_1}{\alpha_2 (m_1 - n_1)} + \frac{2^{(q_1-p_1)/(2q_1)} q_1}{\beta_2 (q_1 - p_1)} + \frac{1}{\alpha_1 \beta_1}. \tag{29}$$

Proof. Differentiating S_1 with respect to time yields

$$\dot{S}_1 = \dot{e}_v + 3\alpha_1 \left(\beta_1 \mathbf{1}_3 + e_p^2\right)^{\frac{1}{2}} \circ e_v \circ |e_p| . \tag{30}$$

Substituting (11), (26), (27), and (28) into (30) yields

$$\dot{S}_1 = -\alpha_2 S_1^{\frac{m_1}{n_1}} - \beta_2 S_1^{\frac{p_1}{q_1}}. \tag{31}$$

Select the Lyapunov candidate function as $V_1 = \frac{1}{2} S_1^{\mathrm{T}} S_1$. According to Lemmas 4 and 5, we have

$$\begin{aligned} \dot{V}_1 &= S_1^{\mathrm{T}} \dot{S}_1 \\ &= -\alpha_2 S_1^{\mathrm{T}} S_1^{\frac{m_1+n_1}{n_1}} - \beta_2 S_1^{\mathrm{T}} S_1^{\frac{p_1+q_1}{q_1}} \\ &\leqslant -\alpha_2 3^{\frac{n_1-m_1}{2n_1}} (2V_1)^{\frac{m_1+n_1}{2n_1}} - \beta_2 (2V_1)^{\frac{p_1+q_1}{2q_1}} \\ &\leqslant -\alpha_2 3^{\frac{n_1-m_1}{2n_1}} 2^{\frac{m_1+n_1}{2n_1}} V_1^{\frac{m_1+n_1}{2n_1}} - \beta_2 2^{\frac{p_1+q_1}{2q_1}} V_1^{\frac{p_1+q_1}{2q_1}}. \end{aligned} \tag{32}$$

According to Lemma 3, V_1 and S_1 will converge to 0 in a fixed time,

$$t_1 \leqslant \frac{(3/2)^{(m_1-n_1)/(2n_1)} n_1}{\alpha_2 (m_1 - n_1)} + \frac{2^{(q_1-p_1)/(2q_1)} q_1}{\beta_2 (q_1 - p_1)}, \tag{33}$$

$$e_v = -\alpha_1 (\beta_1 \mathbf{1}_3 + e_p^2)^{\frac{3}{2}} \circ \operatorname{sgn}(e_p). \tag{34}$$

Select the candidate Lyapunov function as

$$V_2 = \frac{1}{3} (e_p \circ \operatorname{sgn}(e_p))^{\mathrm{T}} (\beta_1 \mathbf{1}_3 + e_p^2)^{-\frac{1}{2}}. \tag{35}$$

Differentiating V_2 with respect to time and substituting (34) into $\dot{V}_2$ yields

$$\begin{aligned} \dot{V}_2 &= \frac{1}{3} \dot{e}_p^{\mathrm{T}} (\beta_1 \mathbf{1}_3 + e_p^2)^{-\frac{3}{2}} \circ ((\beta_1 \mathbf{1}_3 + e_p^2) \circ \operatorname{sgn}(e_p) - e_p^2 \circ \operatorname{sgn}(e_p)) \\ &= \frac{1}{3} \beta_1 \dot{e}_p^{\mathrm{T}} (\beta_1 \mathbf{1}_3 + e_p^2)^{-\frac{3}{2}} \circ \operatorname{sgn}(e_p) \\ &= -\alpha_1 \beta_1. \end{aligned} \tag{36}$$

Since $V_2 \in [0, 1)$, in a fixed time $t_2 = \dfrac{|V_2(0)|}{\alpha_1 \beta_1} \leqslant \dfrac{1}{\alpha_1 \beta_1}$, e_p and e_v will be zero. In summary, e_p and e_v will converge to zero in a fixed time $t \leqslant t_0 + t_1 + t_2$. This concludes the proof.

Remark 5. Comparing (28) with the proposed control in [15], it can be concluded that, the proposed fixed-time control algorithm in this paper is simpler in form and lower in computational complexity. In addition, to resist disturbance, Ref. [15] introduces switching function in control input, while in (26), disturbance estimation $\hat{D}_1$ is introduced instead of sign function. Thereby, the chattering problem in the proposed control input signals is alleviated compared with the result in [15].

4.3 The attitude controller

Let $\Theta_d = [\phi_d, \theta_d, \psi_d]^{\mathrm{T}}$ be the desired Euler angle. If we define $e_\Theta = \Theta - \Theta_d$ and $e_\Omega = W\Omega - \dot{\Theta}_d$, then Eqs. (4) and (5) can be rewritten as

$$\begin{cases} \dot{e}_\Theta = e_\Omega, \\ \dot{e}_\Omega = \tau - F + D_2', \end{cases} \tag{37}$$

where $\tau = WI^{-1}M$, $F = WI^{-1}\Omega \times I\Omega - \dot{W}\Omega + \ddot{\Theta}_d$, and $D_2' = WD_2 = [d_\phi, d_\theta, d_\psi]^{\mathrm{T}}$.

Assumption 2. Suppose that

$$-\frac{\pi}{2} < \phi < \frac{\pi}{2} \text{ and } -\frac{\pi}{2} < \theta < \frac{\pi}{2}.$$

Assumption 3. $d_i(0) = 0$, $|\dot{d}_i| \leqslant L_2$, $i = \{\phi, \theta, \psi\}$, where $L_2 > 0$ is a constant.

4.3.1 *Design of the disturbance observer* $\hat{D}_2$

The disturbance observer is designed as

$$\hat{D}_2 = -k_6 \int_0^t \text{sgn}(\Delta_2) \text{d}\tau, \tag{38}$$

where $\Delta_2 = Y_2 - e_\Omega = [\Delta_{21}, \Delta_{22}, \Delta_{23}]^{\text{T}}$,

$$Y_2 = \int_0^t -k_4 \Delta_2 \|\Delta_2\|^{\mu_2 - 1} - k_5 \Delta_2 \|\Delta_2\|^{\lambda_2 - 1} + \tau - F + \hat{D}_2 \text{d}\tau, \tag{39}$$

$k_4 > \sqrt{2k_6}$, $k_5 > 0$, $k_6 > 4L_2$, $0 < \mu_2 < 1$, and $\lambda_2 > 1$.

Define the estimation error of disturbance as $\tilde{D}_2 = \hat{D}_2 - D_2'$.

Theorem 3. Consider the system (37). Under Assumptions 2 and 3, if the disturbance observer $\hat{D}_2$ is designed as (38), then $\tilde{D}_2$ will converge to zero in a fixed time

$$t_3 = t_{31} + t_{32}, \tag{40}$$

where

$$t_{31} \leqslant \frac{2^{(1-\mu_2)/2}}{k_4(1-\mu_2)} + \frac{2^{(1-\lambda_2)/2}}{k_5(\lambda_2 - 1)}, \tag{41}$$

and

$$t_{32} \leqslant \frac{k_6 + L_2}{(k_6 - L_2)(1 - \sqrt{2k_6}/k_4)} \left(\frac{2^{(1-\mu_2)/2}}{k_4(1-\mu_2)} + \frac{2^{(1-\lambda_2)/2}}{k_5(\lambda_2 - 1)} \right). \tag{42}$$

The proof is similar to the proof of Theorem 1.

4.3.2 *Design of the control input* M

A fixed-time sliding mode surface is designed as

$$S_2 = e_\Omega + \alpha_3 (\beta_3 \mathbf{1}_3 + e_\Theta^2)^{\frac{3}{2}} \circ \text{sgn}(e_\Theta), \tag{43}$$

where $\alpha_3 > 0$ and $\beta_3 > 0$.

τ can be designed as the form of

$$\tau = \tau_{eq} + \tau_* - \hat{D}_2, \tag{44}$$

where

$$\tau_{eq} = F = WI^{-1}\Omega \times I\Omega - \dot{W}\Omega + \ddot{\Theta}_d, \tag{45}$$

$$\tau_* = -\alpha_4 S_2^{\frac{m_2}{n_2}} - \beta_4 S_2^{\frac{p_2}{q_2}} - 3\alpha_3 (\beta_3 \mathbf{1}_3 + e_\Theta^2)^{\frac{1}{2}} \circ e_\Omega \circ |e_\Theta|, \tag{46}$$

$\alpha_4 > 0$, $\beta_4 > 0$, $0 < n_2 < m_2$, $0 < p_2 < q_2$, m_2, n_2, p_2, and q_2 are odd numbers.

M can be obtained from

$$M = IW^{-1}\tau. \tag{47}$$

Theorem 4. If M is designed as (44) and (47), with the fixed-time sliding mode surface S_2 designed as (44), e_Θ and e_Ω will converge to zero in a fixed time without singularity problem. The convergence time is bounded by

$$t \leqslant t_3 + \frac{(3/2)^{(m_2 - n_2)/(2n_2)} n_2}{\alpha_4(m_2 - n_2)} + \frac{2^{(q_2 - p_2)/(2q_2)} q_2}{\beta_4(q_2 - p_2)} + \frac{1}{\alpha_3 \beta_3}. \tag{48}$$

The proof is similar to the proof of Theorem 2.

Table 1 Quadcopter model parameters

Variable	Value	Units
I_{xx}	1.66556×10^{-5}	$N\ s^2/rad$
I_{yy}	1.65717×10^{-5}	$N\ s^2/rad$
I_{zz}	2.92617×10^{-5}	$N\ s^2/rad$

Table 2 Observer parameters

Variable	Value	Variable	Value
k_1	3	k_4	3
k_2	0.5	k_5	0.5
k_3	4	k_6	4
μ_1	0.5	μ_2	0.5
λ_1	2	λ_2	2

Table 3 Controller parameters

Variable	Value	Variable	Value
α_1	5	β_1	0.1
α_2	2	β_2	1
α_3	0.25	β_3	2
α_4	2	β_4	1
m_1	5	n_1	3
m_2	5	n_2	3
p_1	3	q_1	5
p_2	3	q_2	5

5 Simulation and experimental results

5.1 Simulation results

In this subsection, a simulation is conducted to verify the fixed-time convergence of the disturbance observer and the tracking performance of the quadcopter system under the proposed control. The model parameters of the quadcopter, observer parameters, and controller parameters are given in Tables 1–3.

The time-varying disturbance is given by $d_i = 0.5\sin(2t)$, $i = x, y, z, \phi, \theta, \psi$. The desired trajectory is $x_d(t) = 0.5\cos(t)$, $y_d(t) = 0.5\cos(t)$, $z_d(t) = 0.5\cos(t)$, and $\psi_d(t) = 0$.

The simulation results given in Figures 3–6 are the disturbances and their estimations, position tracking error, attitude tracking error, and control input signals, respectively. Figure 3 shows although the real disturbance is vibrating with a large amplitude and a high frequency, the estimation value synchronizes with the real one, indicating the observer tracks the real disturbance with fast converge rate and high accuracy. Figures 4 and 5 indicate the excellent control performance that both position and attitude tracking error converge to zero in about 3 s, less than the upper limits 4 s derived from (29) and (48). It can be observed that the control input signals are nonsingular and smooth in Figure 6, which indicates the chattering is suppressed.

Figures 7 and 8 exhibits a comparison between the proposed method and the fixed-time algorithm employed in [15]. Let $x(0) = 0$ and $x_d(t) = 1$. Particularly, the parameters are subscribed so that the estimation of the upper bound of the convergence time obtained by both algorithms is 4 s. For both algorithms, three cases have been considered with the initial velocity $v_x(0)$ being 3, 6, and 9 m/s, respectively. The results are two groups of curves depicted in Figure 7. It is learned from Figure 7 that the convergence time of all curves is less than 4 s, consistent with the theoretical result. Futhermore, it can be seen that in the same case, the convergence time obtained by the proposed fixed-time control scheme is closer to 4 s than that obtained by [15]. Hence, the estimation of the convergence time provided by the proposed fixed-time control scheme is more accurate. Figure 8 exhibits a comparison between the proposed controller and the fixed-time algorithm employed in [15] in terms of the control input u_1. The time-varying disturbance is assumed as $d_z = 0.5\sin(2t)$. Let $z(0) = -1$, $z_d(t) = 1$, and $v_z(0) = 0$. Particularly, the parameters are subscribed so that the estimation of the upper bound of the convergence time obtained by both strategies is 4 s in theory. It is obtained from Figure 8 that the chattering problem of the control input signals of the proposed fixed-time control scheme is alleviated compared with the

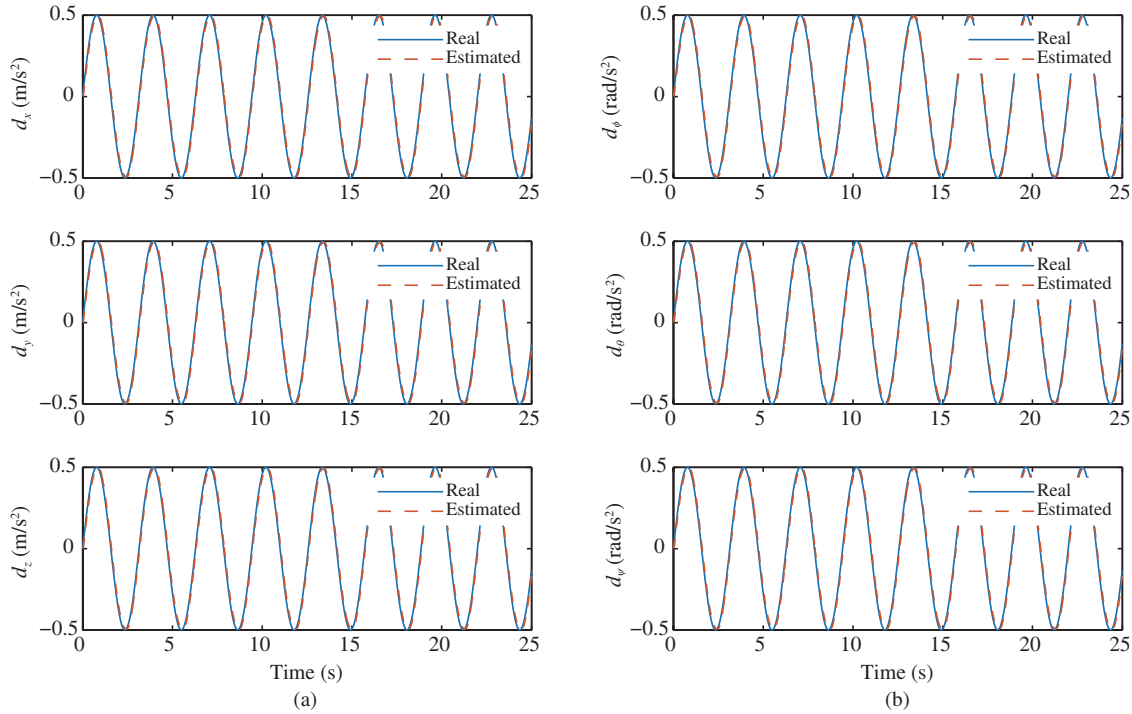

Figure 3 (Color online) The disturbances and their estimations in (a) the translational system and (b) the rotational system.

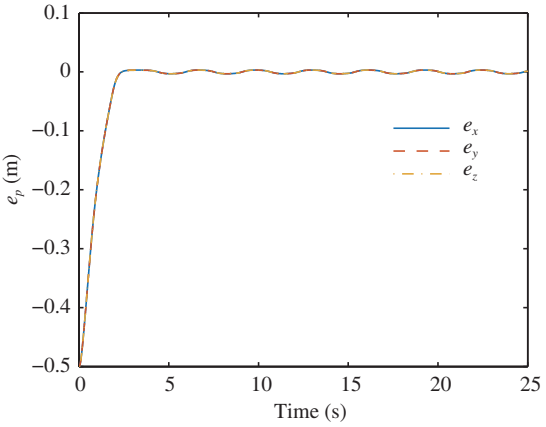

Figure 4 (Color online) Position tracking error.

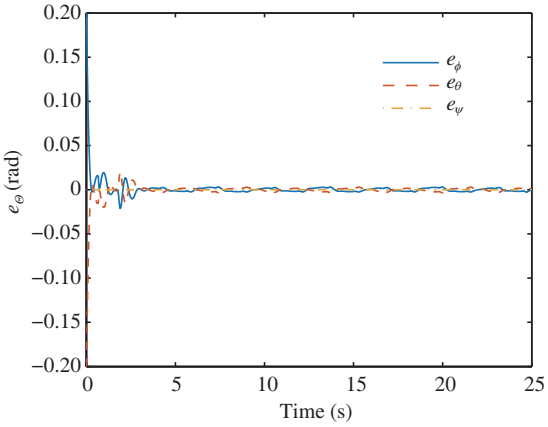

Figure 5 (Color online) Attitude tracking error.

results obtained by [15].

5.2 Experiment setup

The position and attitude tracking experiment has been conducted on Crazyflie 2.0 nano-quadcopter which is an open-source flight platform produced by Bitcraze AB. Carrying many on-board sensors including a 3-axis accelerometer, a 3-axis gyroscope, an optical flow sensor, and a laser ranging device, the nano-quadcopter is able to sense its position, attitude, velocity, and angular velocity. In addition, a wireless module called crazyradio is used to exchange data between the quadcopter and the ground station and achieves real-time control and feedback. The photo of the quadcopter experimental platform is given in Figure 9.

5.3 Experimental results

The desired trajectory is $z_d(t) = 0.25$, $\psi_d(t) = 0$ and

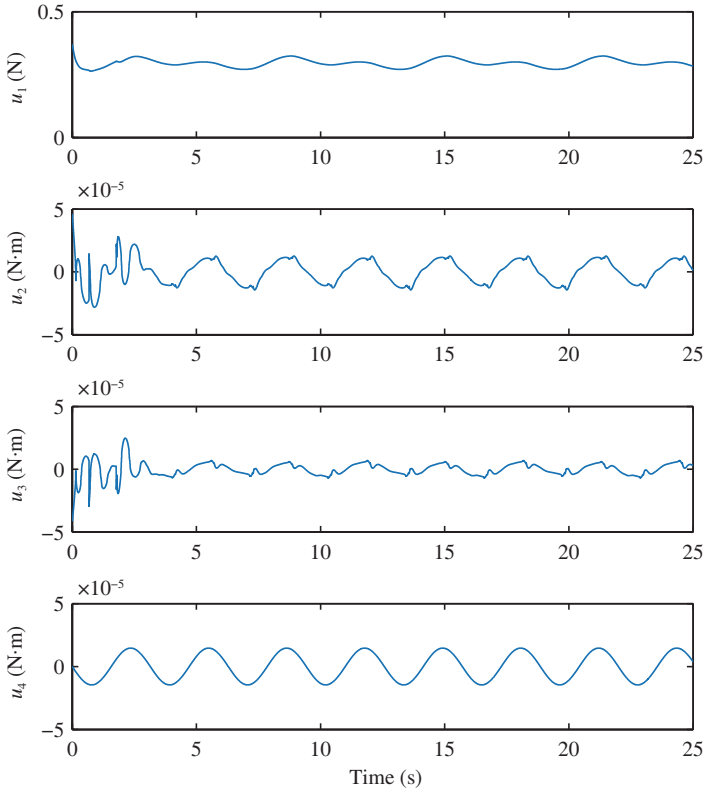

Figure 6 (Color online) Control input signals.

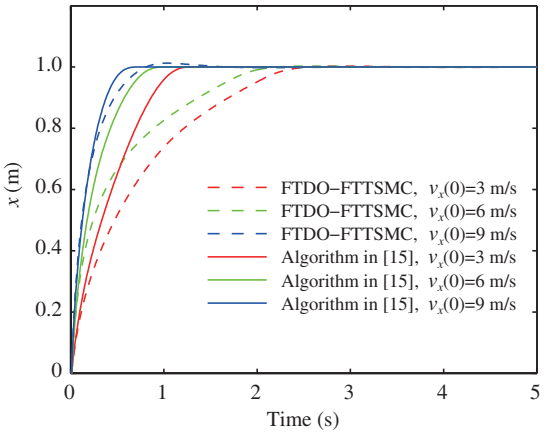

Figure 7 (Color online) Convergence time of FTDO-FTSMC and algorithm in [15].

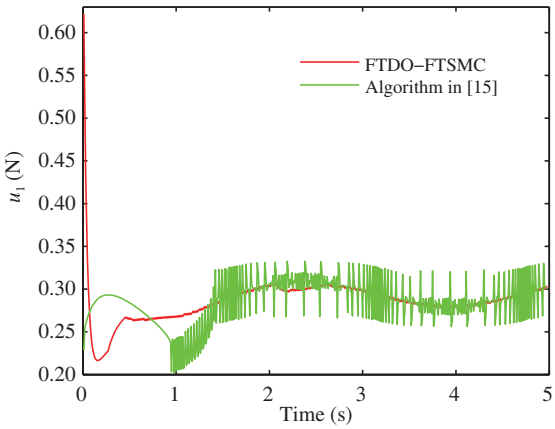

Figure 8 (Color online) Control input of FTDO-FTSMC and algorithm in [15].

$$x_d(t) = \begin{cases} 0, & 0\ \text{s} < t < 5\ \text{s}, \\ 1, & 5\ \text{s} \leqslant t \leqslant 15\ \text{s}, \\ 0, & 15\ \text{s} \leqslant t \leqslant 25\ \text{s}, \end{cases}$$

$$y_d(t) = \begin{cases} 0, & 0\ \text{s} < t < 10\ \text{s}, \\ -1, & 10\ \text{s} \leqslant t \leqslant 20\ \text{s}, \\ 0, & 20\ \text{s} \leqslant t \leqslant 25\ \text{s}. \end{cases}$$

The desired trajectory and the real trajectory of the Crazyflie 2.0 are depicted in Figure 10. The

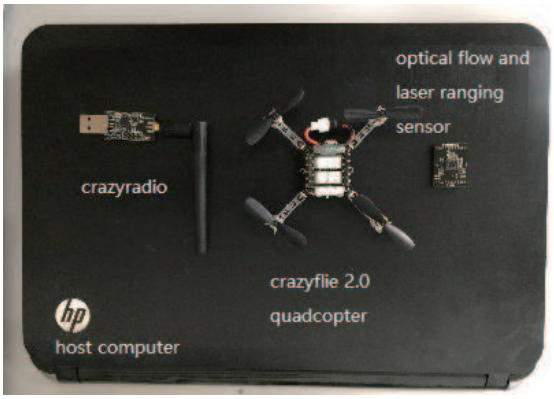

Figure 9 (Color online) Quadcopter experimental platform.

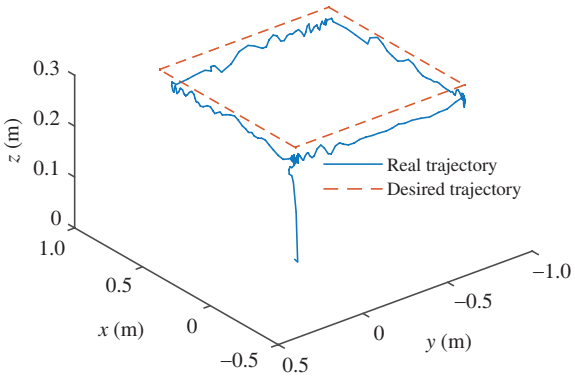

Figure 10 (Color online) The desired trajectory and the real trajectory of the Crazyflie 2.0.

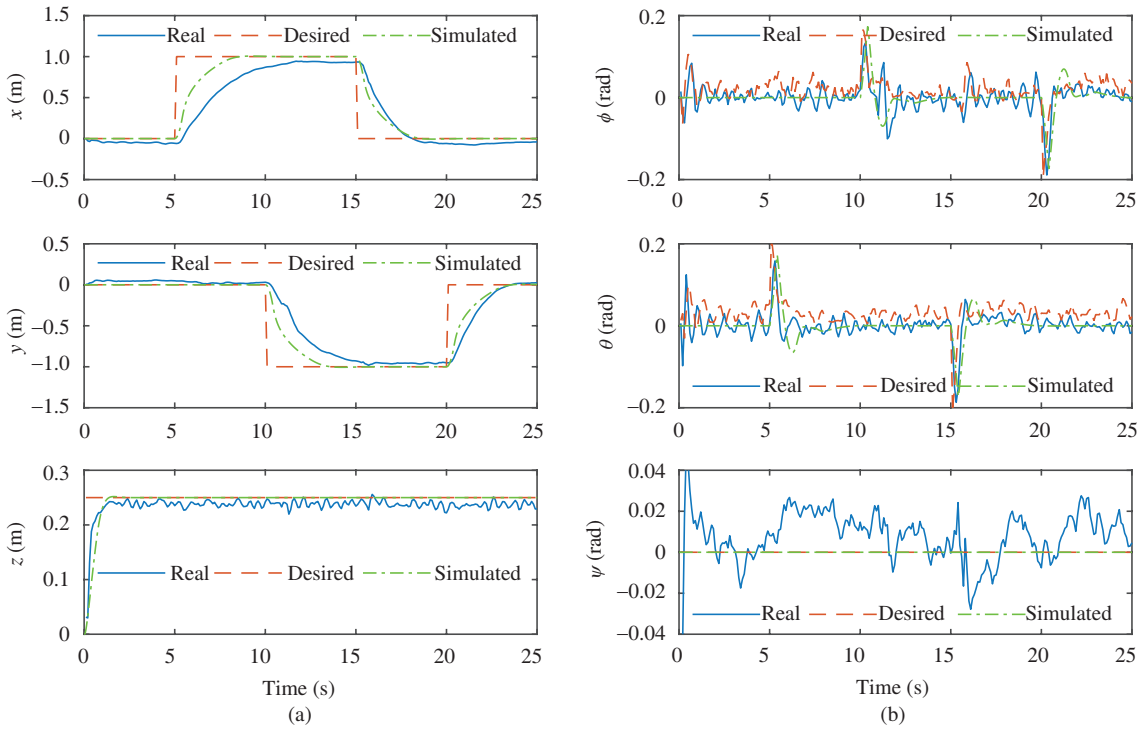

Figure 11 (Color online) Position and attitude of the Crazyflie 2.0. Real, desired and simulation results of (a) the translational motion and (b) the rotational motion.

desired position and attitude and the simulation results as well as the experiment results of the Crazyflie 2.0 are depicted in Figure 11.

It can be noted that, the real trajectory is consistent with the simulation results except for small errors caused by inaccuracy of the sensors and delay caused by input saturation, which validates the fixed-time convergence of the presented algorithm.

6 Conclusion

In this paper, we have developed a disturbance observer-based nonsingular fixed-time sliding mode tracking control algorithm for a quadcopter. With more accurate convergence-time determinations and better chattering alleviation, this control algorithm ensures fixed-time convergence of both position and attitude to the desired trajectories. Using Lyapunov stability analysis, we have presented a rigorous proof of the fixed-time stability of the proposed algorithm. Finally, we have carried out numerical simulations and

experiments to verify the fixed-time tracking performance of the developed method.

Acknowledgements This work was supported in part by the National Natural Science Foundation of China (Grant Nos. 61973133, 61673303, 61633011, 61976099).

References

1 Tripathi V, Behera L, Verma N. Design of sliding mode and backstepping controllers for a quadcopter. In: Proceedings of the 39th National Systems Conference (NSC), Noida, 2015
2 Argentim L, Rezende W, Santos P, et al. PID, LQR and LQR-PID on a quadcopter platform. In: Proceedings of International Conference on Informatics, Electronics and Vision (ICIEV), Dhaka, 2013
3 Xiong J J, Zhang G B. Global fast dynamic terminal sliding mode control for a quadrotor UAV. ISA Trans, 2017, 66: 233–240
4 Tian B L, Liu L H, Lu H C, et al. Multivariable finite time attitude control for quadrotor UAV: theory and experimentation. IEEE Trans Ind Electron, 2018, 65: 2567–2577
5 Xu B. Composite learning finite-time control with application to quadrotors. IEEE Trans Syst Man Cybern Syst, 2018, 48: 1806–1815
6 Alexis K, Nikolakopoulos G, Tzes A. Design and experimental verification of a constrained finite time optimal control scheme for the attitude control of a quadrotor helicopter subject to wind gusts. In: Proceedings of IEEE International Conference on Robotics and Automation, Anchorage, 2010. 1636–1641
7 Polyakov A. Nonlinear feedback design for fixed-time stabilization of linear control systems. IEEE Trans Autom Control, 2012, 57: 2106–2110
8 Zhang Z C, Wu Y Q. Fixed-time regulation control of uncertain nonholonomic systems and its applications. Int J Control, 2017, 90: 1327–1344
9 Parsegov S, Polyakov A, Shcherbakov P. Fixed-time consensus algorithm for multi-agent systems with integrator dynamics. In: Proceedings of the 4th IFAC Workshop on Distributed Estimation and Control in Networked Systems, Koblenz, 2013. 110–115
10 Liu X G, Liao X F. Fixed-time $\mathcal{H}_\infty$ control for port-controlled hamiltonian systems. IEEE Trans Autom Control, 2019, 64: 2753–2765
11 Zuo Z Y. Non-singular fixed-time terminal sliding mode control of non-linear systems. IET Control Theory Appl, 2015, 9: 545–552
12 Corradini M L, Cristofaro A. Nonsingular terminal sliding-mode control of nonlinear planar systems with global fixed-time stability guarantees. Automatica, 2018, 95: 561–565
13 Zuo Z Y. Nonsingular fixed-time consensus tracking for second-order multi-agent networks. Automatica, 2015, 54: 305–309
14 Basin M, Panathula C B, Shtessel Y. Multivariable continuous fixed-time second-order sliding mode control: design and convergence time estimation. IET Control Theory Appl, 2017, 11: 1104–1111
15 Yun H, Zuo Z Y, Shi Z G. Fixed-time terminal sliding mode trajectory tracking control of quadrotor helicopter. In: Proceedings of the 34th Chinese Control Conference (CCC), Hangzhou, 2015. 4361–4366
16 Fu J J, Wang J Z. Fixed-time coordinated tracking for second-order multi-agent systems with bounded input uncertainties. Syst Control Lett, 2016, 93: 1–12
17 Chen M, Shi P, Lim C C. Robust constrained control for MIMO nonlinear systems based on disturbance observer. IEEE Trans Autom Control, 2015, 60: 3281–3286
18 Huang J, Ri S, Fukuda T, et al. A disturbance observer based sliding mode control for a class of underactuated robotic system with mismatched uncertainties. IEEE Trans Autom Control, 2019, 64: 2480–2487
19 Chen W H, Yang J, Guo L, et al. Disturbance-observer-based control and related methods — an overview. IEEE Trans Ind Electron, 2016, 63: 1083–1095
20 Xie W, Yu G, Cabecinhas D, et al. Global saturated tracking control of a quadcopter with experimental validation. IEEE Control Syst Lett, 2021, 5: 169–174
21 Chen F Y, Jiang R Q, Zhang K K, et al. Robust backstepping sliding mode control and observer-based fault estimation for a quadrotor UAV. IEEE Trans Ind Electron, 2016, 63: 5044–5056
22 Cheng X, Liu Z W. Robust tracking control of a quadcopter via terminal sliding mode control based on finite-time disturbance observer. In: Proceedings of the 14th IEEE Conference on Industrial Electronics and Applications (ICIEA), Xi'an, 2019. 1217–1222